

Ultrastructure of Synapses From the Pretectum in the A-Laminae of the Cat's Lateral Geniculate Nucleus

JOSEPHINE B. CUCCHIARO, DANIEL J. UHLRICH, AND S. MURRAY SHERMAN

Department of Neurobiology, State University of New York,
Stony Brook, New York 11794-5230

ABSTRACT

We have recently shown in cats that many neurons projecting to the lateral geniculate nucleus from the pretectum use γ -amino butyric acid (GABA) as their neurotransmitter. We sought to determine the morphology of synaptic terminals and synapses formed by these pretectal axons and the extent to which they resemble other GABAergic terminals found in the geniculate neuropil (i.e., from geniculate interneurons and cells of the nearby perigeniculate nucleus). To do this, we labeled a population of pretectal axons with the anterograde tracer *Phaseolus vulgaris* leucoagglutinin and analyzed the morphology and synaptology of labeled pretectal terminals in the A-laminae of the cat's lateral geniculate nucleus. The pretectal projection, which arises primarily from the nucleus of the optic tract (NOT), provides synaptic innervation to elements in the geniculate neuropil. The labeled NOT terminals are densely packed with vesicles, contain dark mitochondria, and form symmetrical synaptic contacts. These are characteristics of the F1 type of terminal, and we know from other studies that GABAergic axon terminals from interneurons and perigeniculate cells also give rise to F1 terminals. We compared our population of NOT terminals with labeled perigeniculate and unlabeled F1 terminals selected from the geniculate neuropil and found that all three populations share many morphological characteristics. Both qualitative and quantitative assessments of the pretectal terminals suggest that these are a type of F1 terminal. Most pretectal terminals selectively form synapses onto geniculate profiles that contain irregularly distributed vesicles and dark mitochondria and that are postsynaptic to other types of terminals. These postsynaptic targets thus exhibit features of another class of inhibitory, GABAergic terminal known as F2 terminals, which are the specialized appendages of geniculate interneurons. Pretectal inputs, being GABAergic, may thus serve to inhibit local interneuronal outputs. Pretectal axons also innervate the perigeniculate nucleus, in which the only targets are the other main type of inhibitory, GABAergic neurons. These results suggest that the pretectum may facilitate retinal transmission through the lateral geniculate nucleus by providing inhibition to the local inhibitory cells: the interneurons and probably perigeniculate cells. This would serve to release geniculate relay cells from inhibition. © 1993 Wiley-Liss, Inc.

Key words: GABA, NOT, visual system, thalamus, axon terminals

Inputs from the brainstem are important to the control of the transmission of sensory information through the thalamus to the cerebral cortex (for reviews, see Singer, '77; Burke and Cole, '78; Sherman and Koch, '86, '90; Steriade and Llinás, '88). This pathway has been most intensely studied with regard to transmission of retinal signals through the lateral geniculate nucleus in the cat, and the best understood brainstem projection to this thalamic nucleus emanates from cholinergic neurons in the parabrachial region of the brainstem. This input seems to facilitate retinogeniculate transmission both by direct depolarization of relay cells and also by disinhibiting them via direct

hyperpolarization of local inhibitory circuits (McCormick and Prince, '86, '87; McCormick and Pape, '88).

Another input from the brainstem to the lateral geniculate nucleus that has received recent attention derives from the pretectum, mostly from the nucleus of the optic tract (NOT; Graybiel and Berson, '80; Kubota et al., '87, '88;

Accepted March 30, 1993.

Daniel J. Uhrlich's present address is Department of Anatomy, University of Wisconsin, Madison, WI 53706.

Address reprint requests to S.M. Sherman, Department of Neurobiology, State University of New York, Stony Brook, NY 11794-5230.

Cucchiari et al., '91a). This input is particularly interesting, because light microscopic studies suggest that many, and perhaps all, of its underlying axons use γ -aminobutyric acid (GABA) as a neurotransmitter (Cucchiari et al., '91a). We extended these observations by analyzing at the electron microscopic level synaptic terminals labeled from the pretectum.

We pursued several goals with this approach. First, prior studies suggest that GABAergic axon terminals in the geniculate neuropil are of a particular morphological type known as F1 terminals (see Materials and Methods for definitions of F1 and other terminal types), which are thought to be inhibitory (Fitzpatrick et al., '84; Montero and Singer, '85). We sought to extend and confirm the prior light microscopic observations by determining whether or not labeled pretectal terminals are F1 terminals and thereby probably GABAergic. Second, we tried to determine whether the postsynaptic targets of pretectal terminals are relay cells, local inhibitory neurons, or both in order to deduce the functional significance of pretectal input to the lateral geniculate nucleus. Finally, we made a series of quantitative measurements of terminals, synapses, and postsynaptic targets of the pretectum and other sources in order to compare pretectal terminals with others in the geniculate neuropil.

MATERIALS AND METHODS

Many of the new data presented in this paper derive from one adult cat in which we extracellularly injected *Phaseolus vulgaris*-leucoagglutinin (PHA-L) into the pretectum. The PHA-L injection, via anterograde transport, labeled a small population of pretectal axons, which we traced to their terminal arbors and terminals in the lateral geniculate nucleus. For comparison with other terminals of extrinsic origin in the lateral geniculate nucleus, we made use of previously published data (Cucchiari et al., '91b) that include populations of terminals from cortical area 17 and the perigeniculate nucleus labeled with PHA-L and/or horseradish peroxidase (HRP). Finally, from four cats, including one each in which PHA-L was placed into the pretectum or cortical area 17, we analyzed an unlabeled population of terminals.

Abbreviations

F	terminals with flattened or pleomorphic vesicles that form symmetric contacts; most of F terminals are thought to be inhibitory and use GABA as a neurotransmitter
F1	subtype of F terminals that derives from axons and are exclusively presynaptic
F2	subtype of F terminals that derive from dendrites of interneurons and are both presynaptic and postsynaptic
GABAergic	implies that γ -aminobutyric acid is used as a neurotransmitter
LGN	lateral geniculate nucleus
MGN	medial geniculate nucleus
NOT	nucleus of the optic tract
OPN	olivary pretectal nucleus
PHA-L	<i>Phaseolus vulgaris</i> -leucoagglutinin
PGN	perigeniculate nucleus
PPN	posterior pretectal nucleus
RLP	terminals with round vesicles, large profiles, pale mitochondria that form asymmetric contacts and are retinal in origin
RSD	terminals with round vesicles, small profiles, dark mitochondria that form asymmetric contacts and mostly derive from cortex

Bulk labeling with PHA-L

Our methods for PHA-L injection and subsequent preparation of the tissue for electron microscopic analysis have been described previously (Cucchiari et al., '88, '91b) and are presented here in abbreviated form only for the labeling of pretectal terminals, since methods for the labeling of cortical and perigeniculate terminals are reported in Cucchiari et al. ('91b). We anesthetized the cat with sodium pentobarbital administered intravenously (initial dose of 15 mg/kg with 5–10 mg supplements as needed) and placed it a stereotaxic apparatus. Sterile procedures were used for all surgery. We administered atropine sulphate (0.15–0.20 mg) to minimize salivation, infused all wound margins and pressure points with 2% lidocaine, and covered the corneas with contact lenses. Vital signs were continuously monitored.

For the injection into the pretectum, we first aspirated the overlying cortex, and then located the pretectum by visual inspection under an operating microscope. Once exposed, we placed an electrode filled with PHA-L (2.5% in 0.05 M sodium phosphate buffer, pH 7.4) into the pretectum and iontophoretically injected the PHA-L (5 μ A positive current pulsed on and off at 0.07 Hz for 15 minutes). For the 48 hour survival period following the PHA-L injection, anesthesia was continuously maintained.

Tissue processing

After the 48 hour survival period, the cat was deeply anesthetized with an intravenous overdose of sodium pentobarbital and perfused transcardially, first with heparin, then by a brief saline rinse, and finally with aldehyde fixatives (4% paraformaldehyde, 0.05% glutaraldehyde, and 0.1 M sodium phosphate at pH 7.4). After the perfusion, the brain was removed from the skull and a block of tissue containing the thalamus and midbrain was placed in fixative (4% paraformaldehyde in 0.05 M sodium borate buffer at pH 9.5) for 12–18 hours at 4°C.

The day after the perfusion, we used a Vibratome to cut 50 μ m coronal sections. The sections were collected and stored in buffered saline. We then passed the sections through an ethyl alcohol series (10%, 20%, 40%, 20%, 10%) for 10 minutes each and back into buffered saline to enhance penetration of subsequent reagents (Eldred et al., '83). These sections were then incubated with gentle agitation in a solution containing primary antibody directed against PHA-L (goat anti-PHA-L at 1:2,000; 2% normal rabbit serum; 0.02 M potassium phosphate buffer at pH 7.4; Vector Labs; Burlingame, CA) for 72 hours at 4°C. We then used the avidin-biotin immunoperoxidase procedure to visualize the antibody (Vectastain ABC kit). Peroxidase was demonstrated with diaminobenzidine (DAB) and cobalt chloride intensification (Adams, '77).

We mounted the processed sections onto glass slides with buffer and examined them with the light microscope to select the sections with labeled processes. Selected sections were osmicated, dehydrated, and embedded in plastic (Epon). Labeled processes were examined and drawn with a camera lucida attached to a light microscope, fitted with oil immersion lenses, at 500 \times and 1,000 \times .

Electron microscopic analysis

Once blocks were prepared for electron microscopy, serial thin sections were cut, mounted onto formvar-coated, slotted grids, and stained with uranyl acetate and lead

citrate. We subsequently examined and photographed selected areas in the geniculate A-laminae. We examined every section in each of three separate blocks.

We used Guillery's ('69a,b) classification of synaptic profiles in the geniculate A-laminae to distinguish among four types: RLP (round vesicles, large profiles, pale mitochondria) terminals form asymmetric contacts and are retinal in origin; RSD (round vesicles, small profiles, dark mitochondria) form asymmetric contacts and mostly derive from cortex; F1 (flattened or pleomorphic vesicles) terminals derive from axons, form symmetric contacts, and are exclusively presynaptic; and F2 (flattened or pleomorphic vesicles) terminals derive from dendrites of interneurons, form symmetric contacts, and are both presynaptic and postsynaptic. In terminals labeled with PHA-L, the electron-opaque DAB reaction product obscures many features, including presynaptic specializations and cytoplasmic matrix. Although the mitochondria and synaptic vesicles remain unlabeled, vesicle shape, size, and distribution may be affected by the labeling. We have thus relied on the postsynaptic elements to identify the presence and type of synaptic contacts. We identified synaptic contacts by a parallel apposition of the pre- and postsynaptic membranes, some widening of the synaptic cleft, density in the synaptic cleft, a postsynaptic density associated with the contact zone, and the presence of the contact zone in three or more serial sections.

For many terminals, we obtained electron micrographs from a complete series of sections; we printed most of these at magnifications of 27,000, although we also used other magnifications (8,200, 11,800, or 46,000; see below). These serial micrographs permitted a detailed reconstruction of each terminal, and such reconstructions were important for establishing certain other features, as follows: 1) we confirmed whether or not a terminal was postsynaptic, thereby helping to distinguish between F1 and F2 terminals (see above); 2) at a magnification of 27,000, we determined the sizes of terminals by measuring the long and short diameters of each terminal at the site of synaptic contact and averaging these values to arrive at a single measure of terminal diameter; for rare terminals in our sample that made more than one contact, we simply averaged the derived diameter estimates from each contact; 3) at magnifications of 8,200 or 11,800, we used the same method to measure the diameters of postsynaptic targets at the synapse; 4) also at magnifications of 8,200 or 11,800, we measured the longest axis of each synaptic contact zone; 5) at a magnification of 46,000, we measured the extent of postsynaptic density and the width of the synaptic cleft for each contact that was judged to be cut perpendicular to the membranes (Cucchiaro et al., '88); and 6) finally, these same serial micrographs enabled us to reconstruct limited segments of the targets postsynaptic to the terminals under investigation. Where these targets were dendrites, we could also determine the types of other synaptic profiles contacting the common target dendrite.

Statistics

Unless otherwise noted, all statistical comparisons were carried out with the Mann-Whitney *U*-test.

RESULTS

Our observations are based on axons labeled from the pretectal region in one cat. We made a single penetration

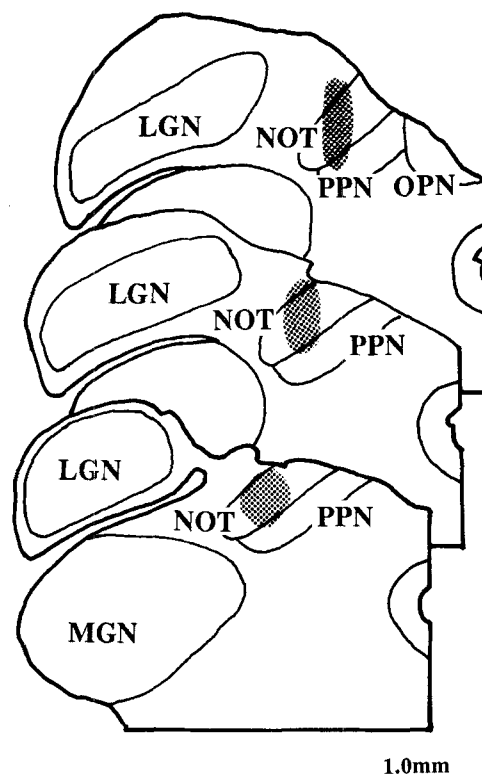


Fig. 1. Reconstruction of three coronal sections through the cat's thalamus and pretectum showing the PHA-L injection site (stippled). The top section is most rostral.

with a microelectrode filled with PHA-L, and we iontophoresed the label at two depths. As shown in Figure 1, the injection was largely limited to the nucleus of the optic tract (NOT), but also encroached slightly into the posterior pretectal nucleus. Because the injections were largely confined to the NOT, we conclude that nearly all of our sample of labeled axons derives from the NOT, and we refer below to the labeled synaptic terminals as NOT terminals. This procedure labeled a small number of axons and terminal arbors in the lateral geniculate nucleus. We concentrated on labeled terminals within the A-laminae. We cannot be certain precisely how many different axons contributed to the sample of synaptic terminals we analyzed.

Light microscopic observations

Labeled NOT axons were sparsely distributed throughout the lateral geniculate nucleus, but were predominantly found in laminae A and A1. The axons had swellings en passant that gave them a beaded appearance. Figure 2 is a photomicrograph of one such axon in lamina A. In addition, although not illustrated here, labeled terminal arbors were found in the perigeniculate nucleus, just dorsal to lamina A. We did not do an electron microscopic analysis of these terminals in the perigeniculate neuropil, but it seems reasonable to conclude that, as well as innervating the lateral geniculate nucleus, NOT axons also innervate the perigeniculate nucleus.

Qualitative electron microscopic observations

As noted above, our electron microscopic analysis included several short segments of labeled axons within

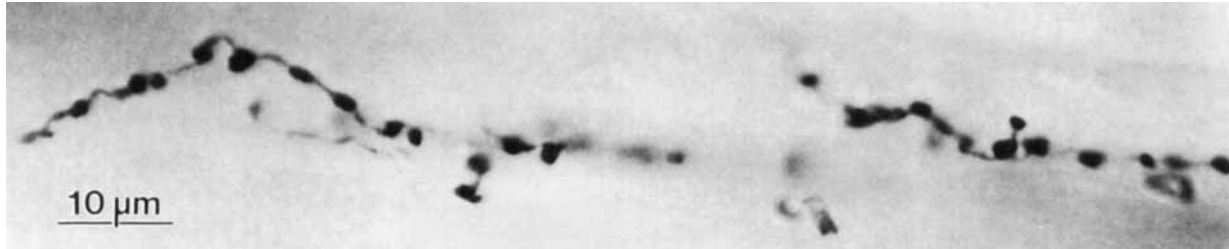


Fig. 2. Photomicrograph of a PHA-L labeled pretectal axon in lamina A of the cat's lateral geniculate nucleus. The axon is beaded, containing a long string of en passant swellings, many of which have been confirmed as sites of synaptic contacts.

laminae A and A1 similar to that illustrated in Figure 2. Overall, we analyzed data from two widely separated blocks containing 31 terminals from 6 separate sprigs of labeled NOT axons. We completely reconstructed these 31 terminals from serial thin sections.

Each of the NOT terminals contained a dense collection of vesicles and dark mitochondria; these vesicles and mitochondria excluded the PHA-L label. Of the 31 terminals, 24 clearly produced synaptic contacts, which was verified by the criteria described in Materials and Methods. However, since these criteria require the observation of synaptic densities and particular apposition of the presynaptic and postsynaptic membranes, it is possible to miss such contact zones if the sectioning were not sufficiently perpendicular through them. That is, obliquely cut synaptic contacts are difficult to recognize in our material. For this reason, we cannot conclude that any of the vesicle-filled swellings lack synaptic outputs, and indeed, it is plausible that all do form synapses. However, our further analysis concentrates on the 24 terminals with identified synaptic outputs. A total of 30 synapses were identified from these labeled NOT terminals. The majority (19) of these terminals had a single synaptic output, some (4) had two synaptic outputs, and 1 had three synaptic outputs. We noticed no difference, including size, between the terminals producing a single synapse and those producing two or three.

All of the synapses from NOT terminals in our sample were symmetrical, with minimal accumulations of postsynaptic dense material (see below). The labeled terminals were exclusively presynaptic: none was found to be postsynaptic to other elements in the geniculate neuropil. These features are characteristic of the F1 class of terminals (Guillery, '69a,b), and all of the NOT terminals in our sample are consistent with this designation.

Figures 3 and 4 illustrate some of the points described above. Figure 3 shows a series of three sections through each of three labeled NOT terminals making synapses onto profiles in the geniculate neuropil. The synaptic contact site for each NOT terminal is shown in several sections as evidence that the postsynaptic density remains thin across the contact zone. Figure 4 shows further examples of labeled NOT terminals forming synaptic outputs in the geniculate neuropil onto profiles that typically contain vesicles. Figure 4A shows a single labeled terminal making three synapses onto three separate profiles, and all of the postsynaptic profiles contain irregularly distributed vesicles. It is worth emphasizing that, because of our serial reconstructions, we can be certain that many or most of these profiles identified as vesicle are indeed spherical and not tubular, as would be the case, for instance, if they were

microtubules cut in cross section. Figure 4B shows a labeled NOT axon making a synapse onto a large geniculate dendrite that also receives an asymmetrical synapse from an unlabeled terminal. This large target dendrite, which contains ribosomes but not vesicles, is particularly noteworthy, because it was the only dendrite of this type (i.e., containing ribosomes but not vesicles, much like a conventional dendrite) to receive a NOT synapse in our sample. Figure 4C–E provides more examples of NOT terminals forming synaptic contacts onto geniculate profiles that contain irregular distributions of vesicles. The vast majority (29 of 30, or 97%) of profiles postsynaptic to NOT terminals thus contain vesicles. Figure 4F shows a low magnification of the geniculate neuropil innervated by an NOT axon.

Not only did most of these postsynaptic targets of NOT terminals contain vesicles, but also our limited reconstructions indicate that they were prominent swellings along rather thin processes, and these are often connected by these thin processes, like beads on a string. No dendritic shafts have yet been described for the cat's lateral geniculate nucleus with these features. Instead, the presence of vesicles in the postsynaptic profiles and their beaded appearance both suggest that these may be dendritic specializations of GABAergic interneurons, because the only vesicle-containing, beaded postsynaptic profiles yet described for the geniculate neuropil are the dendritic outputs of interneurons. These are also called F2 terminals (see Materials and Methods). For the purposes of this description, we shall refer to these as F2-like profiles, because although they resemble typical F2 terminals, there may be some differences (see below).

Figures 5 and 6 are reconstructions of labeled NOT afferents in the lateral geniculate nucleus. Figure 5 depicts terminal processes in lamina A1, and it represents the same material as shown in Figure 4F; Figure 6 depicts terminal processes in lamina A. In each of the reconstructions, every geniculate target of a labeled NOT terminal is a small, vesicle-containing profile. As expected for F2 terminals, these postsynaptic profiles also receive other, unlabeled synaptic inputs, including synapses from RSD, F1, and RLP terminals. Also like F2 terminals, as noted above, these F2-like postsynaptic profiles are connected to each other by exceedingly fine connectives, which makes reconstructing them to other elements generally impractical in our material. We did manage to reconstruct a single example in Figure 5, and the neighboring dendritic swelling formed a symmetrical synaptic output onto a large stem dendrite. This same stem dendrite also received synaptic input from a retinal (RLP) terminal, as did one of the F2-like profiles

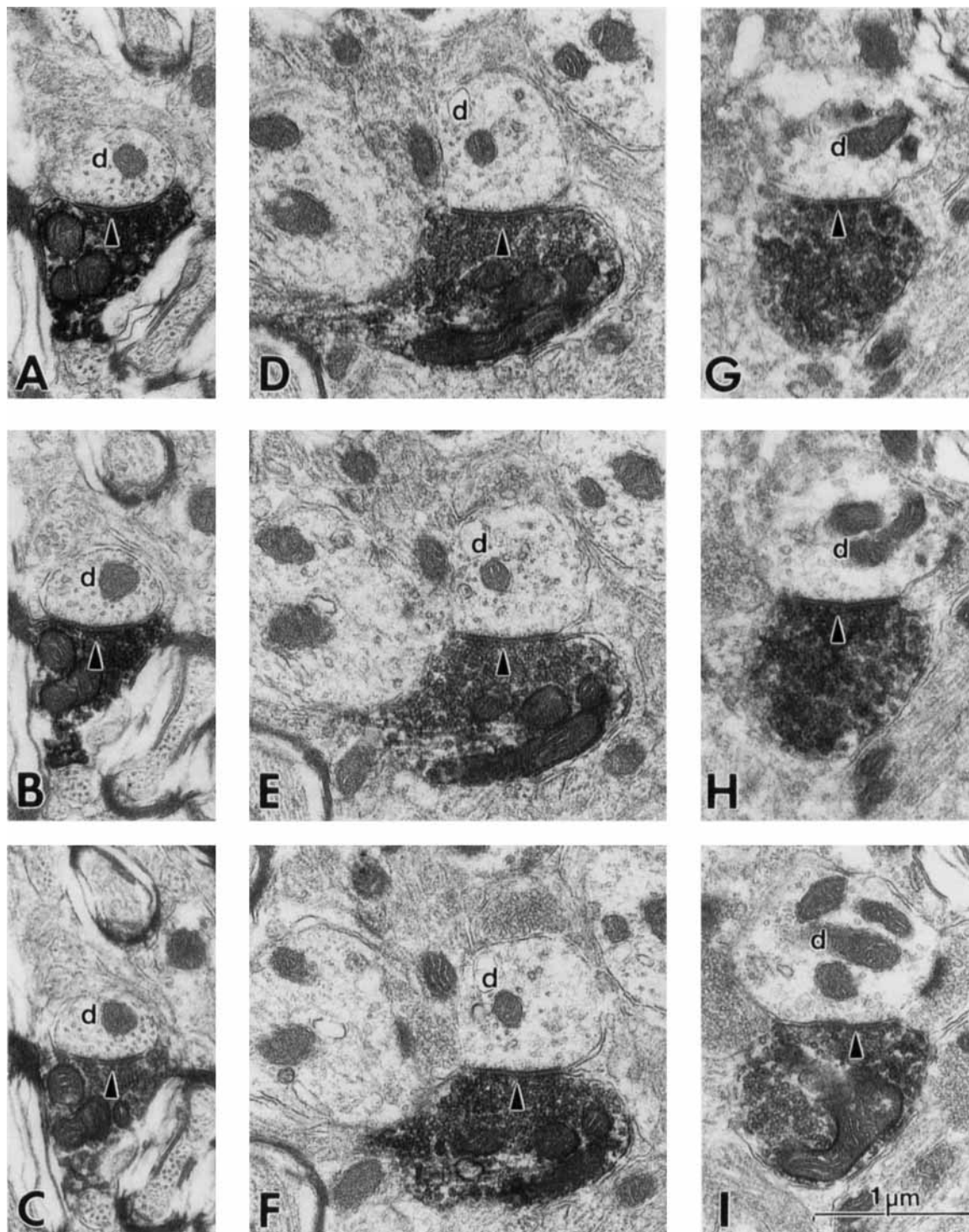


Fig. 3. Electron micrographs of synaptic contacts from PHA-L labeled preterminal axons onto profiles in the geniculate A-laminae. **A-C**: Electron micrographs of three sections through a single synaptic contact (arrowheads) between a darkly labeled preterminal axon terminal and a geniculate profile (d). **D-F**: Series of three sections through another darkly labeled synaptic contact (arrowheads) from a labeled preterminal terminal and an unlabeled geniculate profile (d). **G-I**: Series

of three sections through a third synaptic contact (arrowheads) between a darkly labeled preterminal axon and an unlabeled geniculate profile (d). Note that all three labeled terminals contain dark mitochondria and are filled with synaptic vesicles. Each of the synapses has relatively little postsynaptic density associated with the contact zone, and each exhibits some widening of the synaptic cleft. The scale bar in I also applies to A-H.

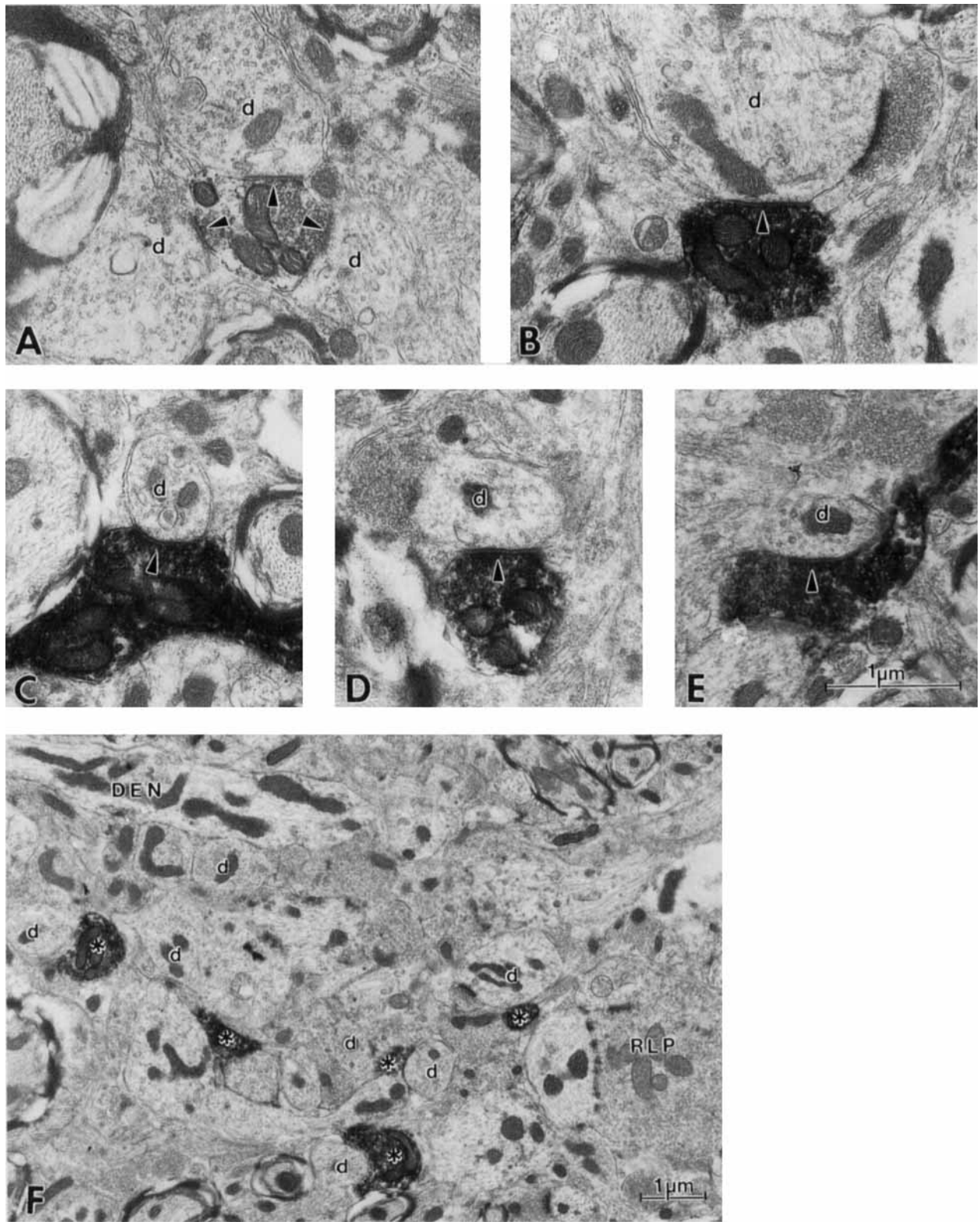


Fig. 4. Electron micrographs of single sections through synaptic contacts from PHA-L labeled preterminal terminals onto geniculate profiles in the geniculate A-laminae. **A:** Lightly labeled preterminal terminal forming three symmetrical synapses (arrowheads) onto separate dendritic elements (d) in the geniculate neuropil. Note that each postsynaptic dendrite contains vesicles. **B:** Unusual example of a preterminal synapse (arrowhead) onto an atypically large geniculate profile (d) containing ribosomes. There was no evidence of vesicles in this profile. This was the only example in our sample of such a dendritic target. **C–E:** Three more examples of labeled preterminal terminals forming symmetrical synapses (arrowheads) onto geniculate profiles (d) that contain vesicles. **F:** Low magnification view of the geniculate neuropil from which the reconstruction in Figure 5 was made. Labeled

preterminal terminals (asterisks) make synapses onto vesicle-containing geniculate profiles (d) in a very complex, dense neuropil. The large stem dendrite (DEN) ultimately receives a symmetrical synapse from a dendritic terminal that was itself postsynaptic to the preterminal axon. Note that the large stem dendrite is studded with vesicle-filled profiles, most of which form synaptic outputs at some level through the reconstruction. The single retinal terminal (RLP) contacts both the stem dendrite and one of the vesicle-containing target profiles. The RLP terminal contains pale mitochondria for comparison with the much darker mitochondria in the other profiles, including the preterminal axons. The scale bar in E also applies to A–D; the scale bar in F applies only to F.



Fig. 5. Serial reconstruction within lamina A1 of a labeled pretectal axon (black) in relation to its postsynaptic target profiles (stippled) and the dendrite postsynaptic to the target profiles (striped). The pretectal axon made nine symmetrical synaptic contacts (black arrowheads from black swellings) onto vesicle-containing profiles. For simplicity, other afferent terminals are not shown, but the profiles postsynaptic to the labeled NOT axons also received synaptic inputs from unlabeled RSD

(solid black dots), F1 (solid black triangles), and RLP (solid black square) terminals. In one instance, the target profile was reconstructed to include a symmetrical synapse onto a large, nearby dendrite (black arrowhead from stippled swelling), which also received inputs from RLP and other terminals (not shown). Figure 4F shows the neuropil from which this reconstruction was made.

postsynaptic to the labeled NOT axon. However, different RLP terminals, perhaps from the same axon, contacted the F2-like profile and stem dendrite. If they were from the same retinal axon, this would provide evidence of a type of triadic retinal circuitry in this pathway, but without further reconstruction we cannot address this issue.

Synaptic triads are characteristic of retinogeniculate circuitry in the X pathway, in which a retinal terminal forms synapses onto both the appendage of an inhibitory geniculate interneuron (an F2 profile) and the dendrite of a geniculate relay cell (Wilson et al., '84; Hamos et al., '87). In turn, the F2 profile forms a synapse onto the same relay cell dendrite, thereby forming a synaptic triad and providing the anatomical basis for feedforward inhibition. Such synaptic circuitry is rare in the Y pathway, with triads typically involving < 10% of the retinal input to geniculate relay cells (Wilson et al., '84).

The vesicle-containing, F2-like profiles postsynaptic to NOT axons may also be involved in retinal triadic circuitry, but this triadic circuitry differs in several important ways from that described above. In our material, the terminal receiving the NOT input does not form a detectable synaptic output. What we did observe is a neighboring terminal attached by a narrow connective that forms the output. A similar arrangement exists for the retinal input to these F2-like profiles. A retinal input is made to both an F2-like profile and the stem dendrite of a presumed geniculate relay cell, but the postsynaptic F2-like profiles rarely form synaptic contacts (see Figs. 5 and 6). The synapse onto the geniculate projection cell arises from a neighboring F2-like profile. This type of input-output relationship may function like the triads common to the X retinogeniculate circuits, but it is anatomically somewhat more complicated, involving several neighboring F2-like profiles to complete the triadic arrangement.

The reconstruction in Figure 6A illustrates a fairly long string of NOT terminals, but we were unable to confirm synaptic outputs for several. In addition to the problem of

missing obliquely cut synaptic contact zones, this may also reflect the lack of a complete reconstruction of these terminals, because they were located very superficially in the tissue block. Illustrated in Figure 6B is a reconstruction of a single NOT synapse onto an F2-like profile that, in turn, does form a synapse. This was the only confirmed example we found of a postsynaptic F2-like profile that directly formed a synapse.

Quantitative electron microscopic observations

Our qualitative observations suggest that NOT terminals are a source of F1 terminals and that their chief target may be F2 terminals of geniculate interneurons. To study this more quantitatively, we have compared various parameters of these profiles with other populations of F1 terminals. We have also measured other terminals from the geniculate neuropil for comparison: we include RSD terminals to emphasize the F1 identity of the labeled NOT terminals, and we include F2 terminals to compare with the postsynaptic profiles of labeled NOT terminals. The nature of our reconstructions, which occasionally included somewhat obliquely cut synaptic contact zones, required us to eliminate some terminals from certain quantitative analyses; thus different numbers appear in some of the comparisons below.

Diameter of synaptic terminals. We compared the labeled NOT terminals with two different populations of F1 terminals: axon terminals labeled from the perigeniculate nucleus, and unlabeled F1 terminals found in the geniculate neuropil as identified by Guillery's ('69a,b) criteria (see Materials and Methods). We had previously shown that perigeniculate terminals are a major source of F1 terminals (Cucchiaro et al., '91b), and, for comparison, we used this previously published material, which included perigeniculate terminals labeled with PHA-L (as in the present study) or via intracellular injection of HRP. The unlabeled F1

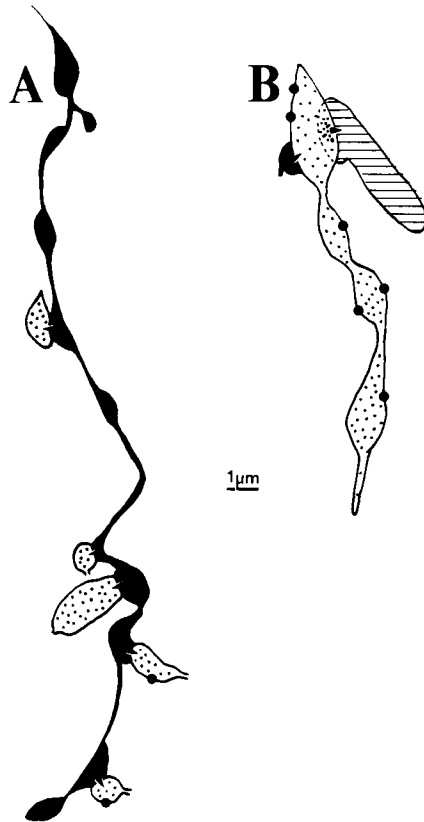


Fig. 6. Serial reconstructions of labeled prepectal axons (solid black) in relation to their postsynaptic target profiles (stippled) and the dendrite postsynaptic to the target profile (striped). Synapses from labeled NOT terminals and from the profiles postsynaptic to NOT terminals are indicated by arrowheads; solid black circles indicate contacts from unlabeled RSD terminals onto the target profiles. **A:** Segment of prepectal axon with 11 swellings, 5 of which made symmetrical synaptic contacts onto vesicle-containing dendritic profiles in the neuropil. The remaining swellings did not have identified synaptic outputs; we interpret this to result from their location at the surface of the tissue block and our inability to reconstruct them completely. The general organization of the neuropil from which this axon was reconstructed is very similar to that shown in Figure 4F, except this was from a block of tissue in lamina A, well rostral to the reconstruction shown in Figure 5. Like the neuropil in Figure 4F, a large stem dendrite studded with vesicle-containing terminals passed through the region, but we were unable to connect any of the small target profiles to those contacting the stem dendrite. **B:** Single labeled prepectal terminal formed a synapse onto a vesicle-containing profile that, in turn, made a symmetrical synaptic contact onto another dendrite.

terminals are presumably of mixed origin. They thus likely include unlabeled terminals from the perigeniculate nucleus and the NOT as well as from other sources, such as axon terminals of interneurons (Montero, '87) and terminals from regions of the thalamic reticular nucleus other than the perigeniculate nucleus (Cucchiario et al., '90).

Figure 7 illustrates the distribution of terminal diameters measured from labeled NOT (Fig. 7A), labeled perigeniculate (Fig. 7B), and unlabeled F1 terminals selected randomly from the neuropil of the geniculate A-laminae (Fig. 7C). It is worth noting that the sample of labeled perigeniculate terminals derives from our recently published study (Cucchiario et al., '91b) that used both HRP and PHA-L to label these terminals, and we found no

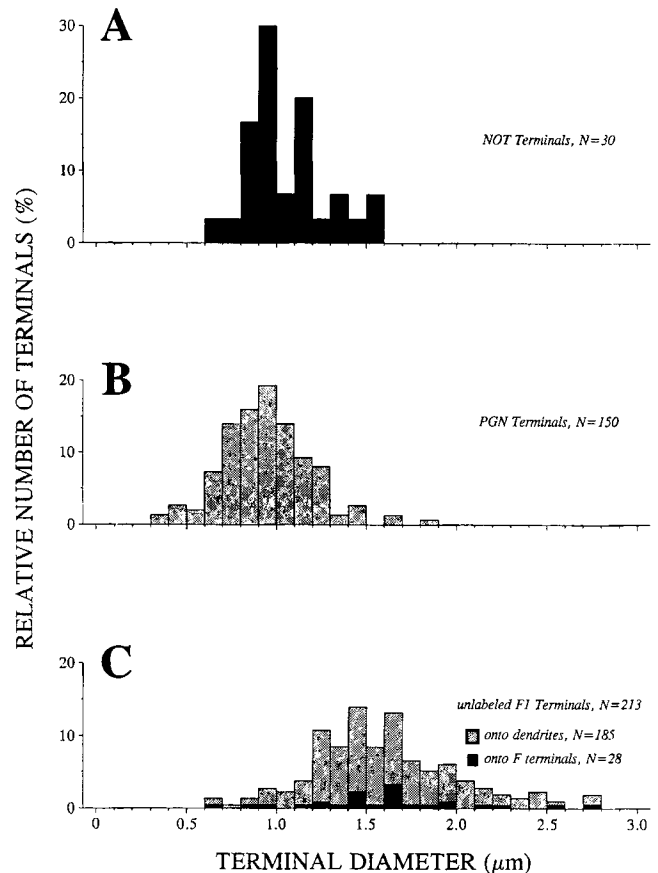


Fig. 7. Frequency histograms associated with various F1 terminal populations. **A:** Labeled terminals from the NOT. **B:** Labeled terminals from the PGN (data from Cucchiario et al., '91b). **C:** Unlabeled F1 terminals. These are further divided into those contacting dendrites and those contacting F terminals; the latter include unambiguous F2 terminals and the F2-like profiles contacted by NOT axons.

differences in any variable due to the two different forms of labeling. We thus feel that comparisons between terminals labeled by HRP and PHA-L are valid. The NOT terminal diameters fall well within the size range of the general population of unlabeled F1 terminals, but, on average, they are smaller ($1.06 \pm 0.22 \mu\text{m}$ versus $1.60 \pm 0.45 \mu\text{m}$; $P < 0.001$). Likewise, as we have reported earlier (Cucchiario et al., '91b), diameters of identified perigeniculate terminals fall within the range of unlabeled F1 terminals, but they, too, are smaller on average ($0.95 \pm 0.25 \mu\text{m}$ versus $1.60 \pm 0.41 \mu\text{m}$; $P < 0.001$). Finally, while the two identified F1 terminal populations, NOT and perigeniculate, have overlapping terminal diameter ranges, the diameters of the NOT terminals are, on average, larger ($P < 0.01$).

Another distinction can be made between NOT and perigeniculate terminals: nearly all of the postsynaptic targets of NOT terminals are F2-like profiles (see above), while none of the perigeniculate targets are (Cucchiario et al., '91b). Figure 7C shows our further analysis of the unlabeled F1 terminals divided into those contacting dendrites ($n = 185$) and those contacting F2-like profiles ($n = 28$). We found no difference in the terminal diameters for these two subsets contacted by unlabeled F1 terminals ($1.59 \pm 0.40 \mu\text{m}$ for dendritic targets and $1.60 \pm 0.45 \mu\text{m}$ for F2-like targets; $P > 0.1$). Furthermore, both subsets of

F1 terminals are larger than their labeled counterparts: the unlabeled F1 terminals contacting dendrites are larger than perigeniculate terminals, and the unlabeled F1 terminals contacting F2-like profiles are larger than NOT terminals ($P < 0.001$ for both comparisons). Thus the size difference between NOT and perigeniculate terminals is not related to their different dendritic or F2-like postsynaptic profiles.

Measurements of synaptic contacts

Postsynaptic density. Of the four terminal types seen in the geniculate neuropil (Guillery, '69a,b), the RLP (retinal) and F2 types are readily identified: RLP terminals are large and have pale mitochondria that are readily distinguished; F2 terminals are the only ones that are postsynaptic, which makes their identification straightforward. What remains is the distinction between F1 and RSD terminals. The key measure here is the postsynaptic density of their contacts, since F1 terminals form symmetric synapses, and RSD terminals form asymmetric synapses (Guillery, '69a,b; Cucchiaro et al., '88, '91b). Figure 8 summarizes the postsynaptic densities of various synaptic contacts from the subset of F1 and RSD terminals in our sample that were cut sufficiently perpendicular to the contact zone to derive these measurements. Shown here are various F1 terminals, including NOT terminals (Fig. 8A), perigeniculate terminals (Fig. 8B), and unlabeled F1 terminals (Fig. 8C); for comparison, we also show two populations of asymmetric terminals, including terminals identified as cortical via PHA-L injections into cortical area 17 (Fig. 8D) and unlabeled RSD terminals (Fig. 8E).

A consistent feature of synapses from F1 terminals is the narrow postsynaptic specialization, which contrasts to the thicker density associated with cortical and many RSD terminals. The unlabeled RSD population shows the most variability, which may reflect multiple sources of RSD terminals. Clearly, the NOT terminals form asymmetric synapses, since their densities are comparable to those of perigeniculate and unlabeled F1 terminals (21.5 ± 2.1 nm for NOT terminals, 24.1 ± 3.0 nm for perigeniculate terminals, and 22.0 ± 3.0 nm for unlabeled F1 terminals; for all pairwise comparisons, $P > 0.1$), and they are much smaller than those of cortical or unlabeled RSD terminals (49.9 ± 4.2 nm for cortical terminals and 47.2 ± 7.3 nm for unlabeled RSD terminals; for all appropriate comparisons, $P < 0.001$). This finding further supports the view that the NOT is a source of F1 terminals to the cat's lateral geniculate nucleus.

Of interest are subtle differences in postsynaptic density among the F1 terminals (Fig. 8A–C). There is no difference, on average, between synaptic densities formed by NOT and unlabeled F1 terminals ($P > 0.1$), but those formed by the perigeniculate terminals are thicker than those formed either by NOT terminals ($P < 0.001$) or by unlabeled F1 terminals ($P < 0.02$). This finding again points to morphological differences among different subsets of F1 terminals. Also of interest, although not a main thrust of this report, is the difference between the subset of RSD terminals identified as cortical in origin (Fig. 8D) and the larger population of unlabeled RSD terminals (Fig. 8E). While the cortical terminals form synapses with postsynaptic densities within the range of those formed by unlabeled RSD terminals, the former do, on average, form larger postsynaptic densities ($P < 0.05$), suggesting that, much like F1 terminals, different subsets of RSD terminals (e.g., from different afferent sources) may differ morphologically.

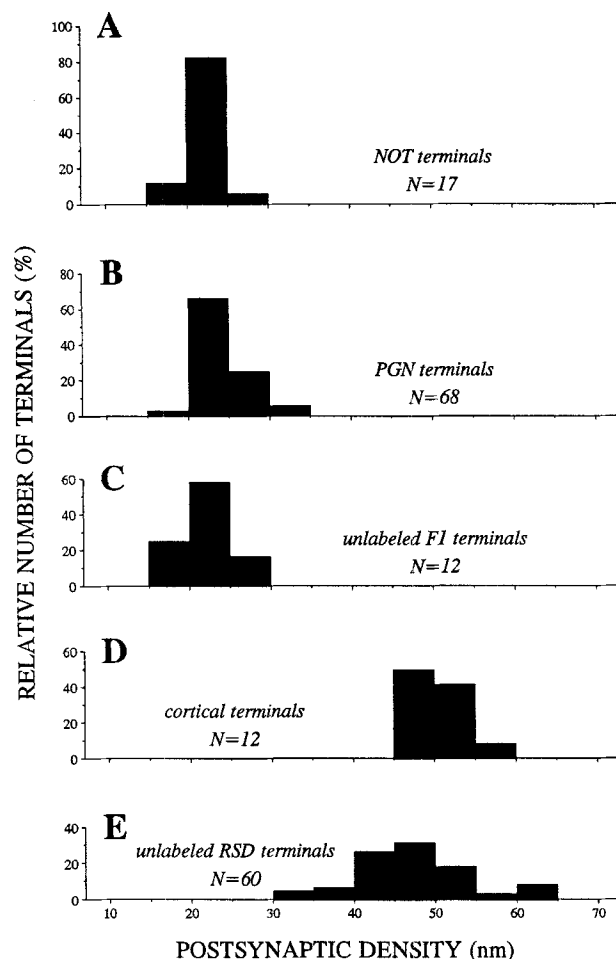


Fig. 8. Frequency histograms of postsynaptic densities associated with synapses from various terminal populations. **A:** Labeled terminals from the NOT. **B:** Labeled terminals from the PGN (data from Cucchiaro et al., '91b). **C:** Unlabeled F1 terminals. **D:** Labeled terminals from the striate cortex (data from Cucchiaro et al., '91b). **E:** Unlabeled RSD terminals.

Length of contact zone. Another feature of many symmetrical synapses is their relatively long synaptic contact zones (Guillery, '69a,b). For a subset of our population, we measured these contact zones, and these data are shown in Figure 9. The analysis includes labeled NOT terminals (Fig. 9A; 583.1 ± 115.0 nm), labeled perigeniculate terminals (Fig. 9B; 491.4 ± 134.1 nm), and a population of unlabeled F1 terminals (Fig. 9C; 635.5 ± 256.7 nm). We found that contact lengths for NOT and perigeniculate terminals are within the range of F1 terminals. A closer inspection reveals that perigeniculate terminals form synapses with the shortest contact zones among F1 terminals, being shorter, on average, than those of either NOT or unlabeled F1 terminals ($P < 0.001$ for both comparisons). NOT terminals form contacts that are in the midrange of lengths for F1 terminals, and there is no difference in their average contact lengths ($P > 0.1$). Finally, some unlabeled F1 terminals have quite long contact sites ($> 1 \mu\text{m}$) that, in our material, remain unlabeled from either the NOT or the perigeniculate nucleus.

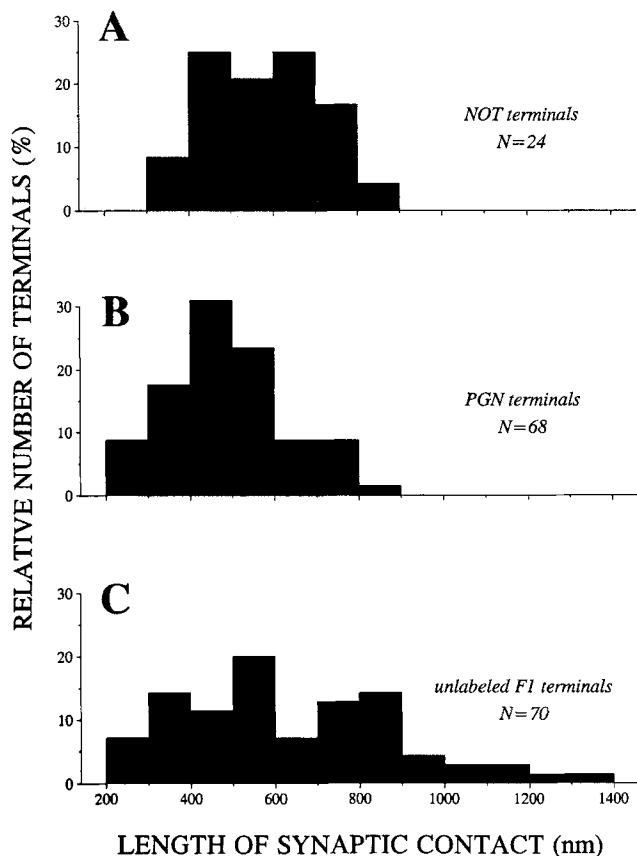


Fig. 9. Frequency histograms of synaptic contact lengths associated with various F1 terminal populations. **A**: Labeled terminals from the NOT. **B**: Labeled terminals from the PGN (data from Cucchiari et al., '91b). **C**: Unlabeled F1 terminals.

Postsynaptic targets. Figure 10 shows the diameters of targets postsynaptic to NOT terminals (Fig. 10A; $0.96 \pm 0.41 \mu\text{m}$), perigeniculate terminals (Fig. 10B; $1.15 \pm 0.53 \mu\text{m}$), and unlabeled F1 terminals (Fig. 10C; $1.57 \pm 0.62 \mu\text{m}$). We could not accurately measure one of the targets of NOT terminals, because it was located near the edge of the block sectioned for electron microscopic analysis; thus only 29 targets were measured. In keeping with our earlier observations that NOT and perigeniculate terminals are subsets of F1 terminals, the size ranges of their postsynaptic targets fall within the range of those of unlabeled F1 terminals. However, the unlabeled population includes a range of targets larger than those seen postsynaptic to either NOT terminals or perigeniculate terminals. Thus, on average, the unlabeled F1 terminals contact larger profiles ($P < 0.001$ for both comparisons). Finally, NOT terminals contact smaller profiles than do perigeniculate terminals ($P < 0.01$).

The difference in size between NOT and perigeniculate targets is consistent with our observation that the target profiles are different: NOT terminals contact mainly F2-like profiles, while perigeniculate terminals contact conventional dendrites or their appendages (Cucchiari et al., '91b). Because the NOT targets are F2-like profiles, we analyzed postsynaptic F2 profiles broken down according to their afferent input (illustrated in Fig. 11). Shown are the F2-like profiles postsynaptic to labeled NOT terminals (Fig.

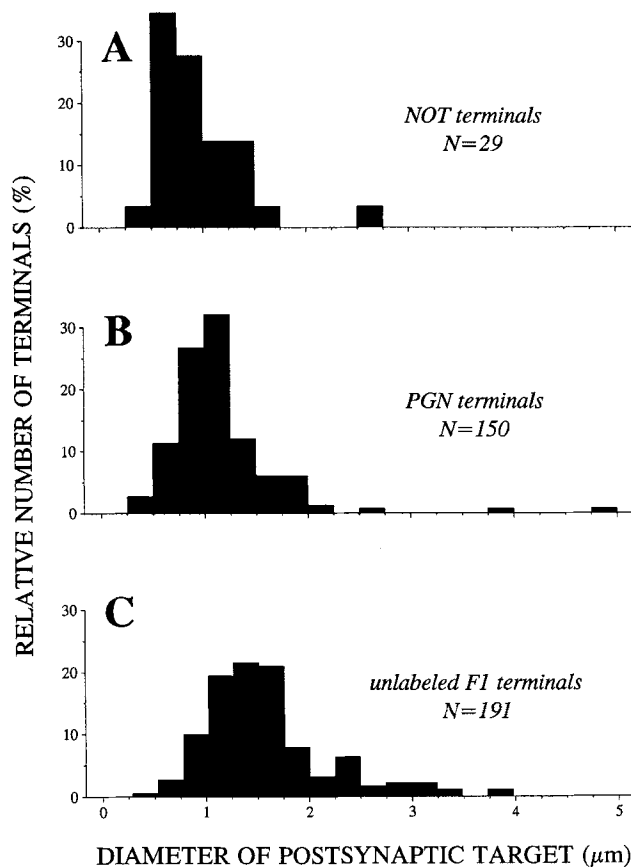


Fig. 10. Frequency histograms of diameters of postsynaptic targets associated with various F1 terminal populations. **A**: Labeled terminals from the NOT. **B**: Labeled terminals from the PGN (data from Cucchiari et al., '91b). **C**: Unlabeled F1 terminals.

11A; $0.96 \pm 0.41 \mu\text{m}$), those postsynaptic to unlabeled F1 terminals (Fig. 11B; $1.26 \pm 0.37 \mu\text{m}$), those postsynaptic to RSD and RLP (retinal) terminals (Fig. 11C; $1.06 \pm 0.27 \mu\text{m}$), and those postsynaptic to all unlabeled terminals (Fig. 11D; $1.15 \pm 0.33 \mu\text{m}$), which combines the populations shown in Figure 11B,C.

Figure 11 shows that the F2-like profiles receiving NOT input are in the same general size range as those receiving inputs from unlabeled F1 terminals, and both of these size ranges overlap that of F2-like profiles receiving input from other types of afferent input. This is consistent with the conclusion that all of these postsynaptic profiles, including those innervated by labeled NOT terminals, are indeed F2 terminals. However, there are differences among the sizes of these postsynaptic profiles. Those innervated by the NOT are smaller than either of those innervated by unlabeled terminals, whether F1 terminals ($P < 0.001$) or RSD and RLP terminals ($P < 0.02$). Furthermore those innervated by unlabeled F1 terminals are larger than those innervated by unlabeled RSD and RLP terminals ($P < 0.01$). This finding suggests that different subpopulations of F2 terminal may be identified based on their different afferent inputs, a point considered further in the Discussion.

Independence of measures. One question we wished to address was whether various pairs of parameters measured

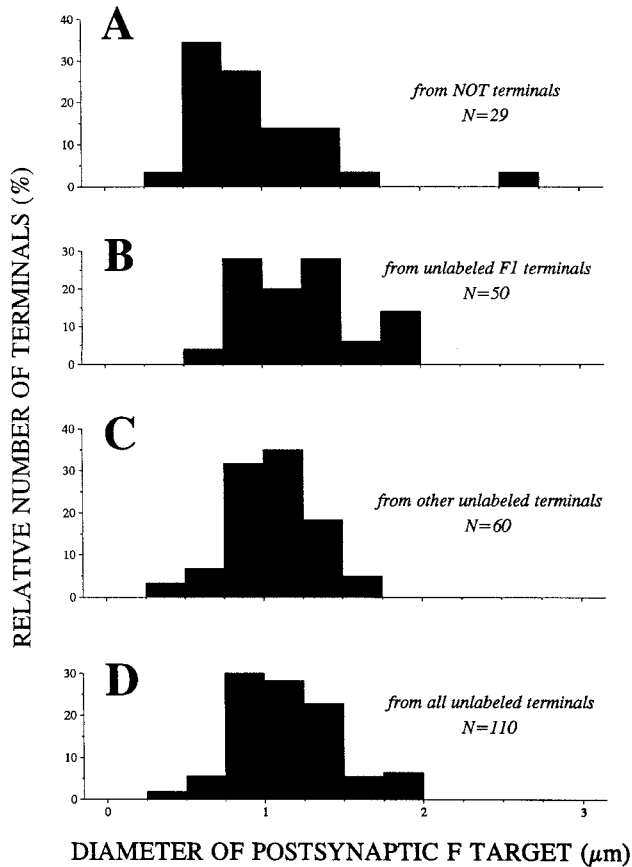


Fig. 11. Frequency histograms of diameters of F2-like profiles postsynaptic to various terminals. **A**: Labeled terminals from the NOT. **B**: Unlabeled F1 terminals. **C**: Unlabeled terminals other than F1 terminals. **D**: All unlabeled terminals. D is a simple sum of B and C.

above for NOT terminals are correlated. On the one hand, correlations could provide insights into ultrastructural relationships, and on the other, lack thereof implies independence of measures, which makes each more significant. A plausible correlation might be diameter of terminal and/or postsynaptic profile versus length of synaptic contact: a larger terminal or profile might promote a longer contact zone. Figure 12 illustrates these relationships, which show little correlation. Figure 12A shows the relationship between contact length and terminal diameter for NOT terminals ($r = 0.00$, $P > 0.1$), perigeniculate terminals ($r = +0.01$, $P > 0.1$), unlabeled F1 terminals contacting dendrites ($r = +0.37$, $P < 0.01$), and unlabeled F1 terminals contacting F2-like profiles ($r = -0.33$, $P > 0.1$). Figure 12B shows the analogous relationship between contact length and diameter of the postsynaptic profile for NOT terminals ($r = 0.00$, $P > 0.1$), perigeniculate terminals ($r = +0.16$, $P > 0.1$), unlabeled F1 terminals contacting dendrites ($r = +0.01$, $P > 0.1$), and unlabeled F1 terminals contacting F2-like profiles ($r = -0.77$, $P < 0.01$). The two plots in Figure 12 are based on slightly different numbers of observations, because, as noted above, not every parameter could be measured for every terminal.

In addition to the analysis summarized by Figure 12, we also tested for correlations between the diameters of terminals and their postsynaptic profiles for the four kinds of

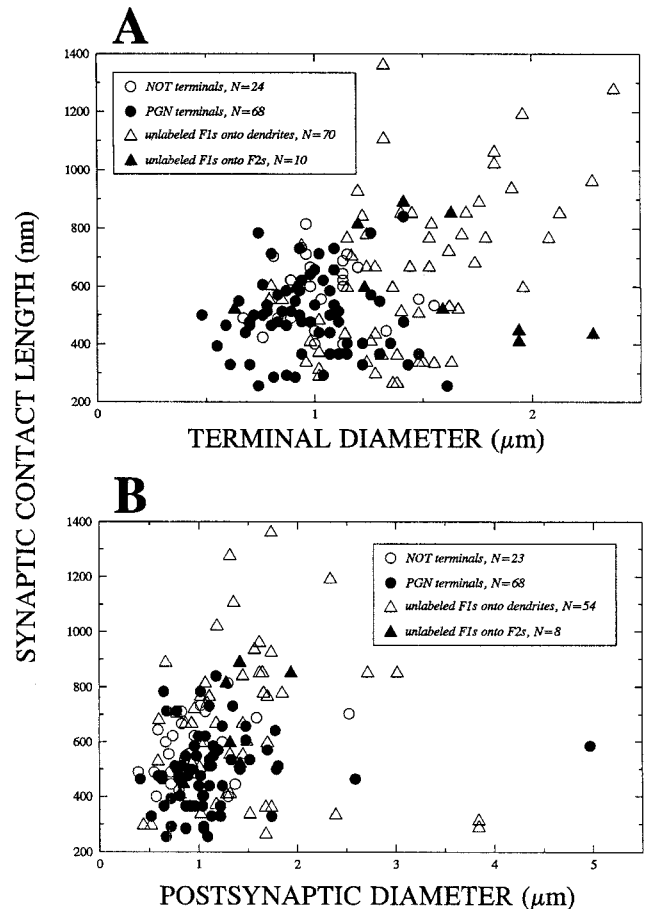


Fig. 12. Scatterplots showing relationships or lack thereof between various parameters for different synaptic terminal populations. **A**: Scatterplot of synaptic contact length versus terminal diameter. **B**: Scatterplot of synaptic contact length versus postsynaptic diameter.

synaptic contact seen (i.e., from NOT terminals, perigeniculate terminals, unlabeled F1 terminals onto dendrites, and unlabeled F1 terminals onto F2-like profiles). We found no significant correlations for any of these combinations. Although Figure 12 suggests correlations for certain terminal and target combinations, none exist that involve NOT terminals. We conclude that, at least for NOT terminals, the measures we have made are reasonably independent of one another.

DISCUSSION

Our results indicate that axons from the NOT innervate the lateral geniculate and perigeniculate nuclei, confirming earlier observations (Graybiel and Berson, '80; Kubota et al., '87, '88; Cucchiaro et al., '91a). Our new observations demonstrate that synaptic contacts formed by these axons derive from F1 terminals, and thus they contribute to a subset of this class of terminals. We also found that the postsynaptic targets of the vast majority of these NOT terminals are F2-like profiles, which are likely to be specialized dendritic terminals of interneurons. An important proviso to these conclusions is that our sample of labeled terminals and axons is small, and it is not yet clear the extent to which these observations can be extrapolated to

the entire projection of the NOT to the lateral geniculate nucleus.

Nature of NOT terminals

Clearly, our labeled NOT terminals fit into the F1 category of terminals. F1 terminals are an important group that represents roughly one-fourth of the synaptic terminals in the A-laminae of the lateral geniculate nucleus (Guillery, '69a,b; Wilson et al., '84). It is not clear from our data what percentage of F1 terminals are represented by the NOT afferents, but our quantitative data, based on analyses of terminal diameter, postsynaptic targets, and synaptic contact morphology (Figs. 7–11), suggest that they are a unique subset different from both unlabeled F1 terminals and another identified population of F1 terminals that emanate from the perigeniculate nucleus. Interestingly, some of the unlabeled F1 terminals have parameters suggesting that they cannot be of perigeniculate or NOT origin: they are too large (Fig. 7) and have synaptic contact zones that are too long (Fig. 9). Other sources of F1 terminal that could contribute to these terminals include axons of interneurons (Montero, '87), axons from regions of the thalamic reticular nucleus other than the perigeniculate nucleus (Cucchiari et al., '90), and axons from the parabrachial region of the brainstem (Cucchiari et al., '88).

Prior work has demonstrated that F1 terminals in the geniculate neuropil are generally GABAergic (Fitzpatrick et al., '84; Montero and Singer, '85). This is consistent with earlier light microscopic observations that the NOT provides a GABAergic input to the lateral geniculate nucleus, that is, roughly 40% of NOT cells retrogradely labeled by HRP injections into the lateral geniculate nucleus were double labeled with an antibody directed against GABA, and this 40% value for GABAergic projection cells from the NOT to the lateral geniculate nucleus was thought to be a conservative estimate (Cucchiari et al., '90).

Postsynaptic targets of NOT terminals

Nearly all of our population of labeled NOT terminals innervate F2-like profiles. As noted in Results, these profiles share many features with F2 terminals: they are vesicle filled, are of the same size range as F2 terminals (Fig. 11), are connected by fine processes generally too thin to reconstruct, and are postsynaptic to other terminals. F2 terminals also form synaptic outputs, but we were unable to confirm this for most of the F2-like profiles postsynaptic to labeled NOT terminals. However, as we noted in Results, failure to find a synaptic contact site is negative evidence that is flawed by the difficulty in seeing these sites if they are obliquely cut. This is consistent with prior analysis from this laboratory of interneurons intracellularly labeled with HRP, of which not every identified F2 terminal had a detectable synaptic output (Hamos et al., '85). Furthermore, only F2 terminals in the lateral geniculate nucleus are known to be vesicle filled, connected by thin processes, and postsynaptic to other terminals. We thus conclude provisionally that the postsynaptic targets of nearly all of our labeled NOT terminals are F2 terminals (see also below). However, we emphasize in the strongest possible terms that our failure to identify synaptic outputs for most of these profiles raises the possibility that they are not F2 terminals and may be some as yet unrecognized type of postsynaptic structure.

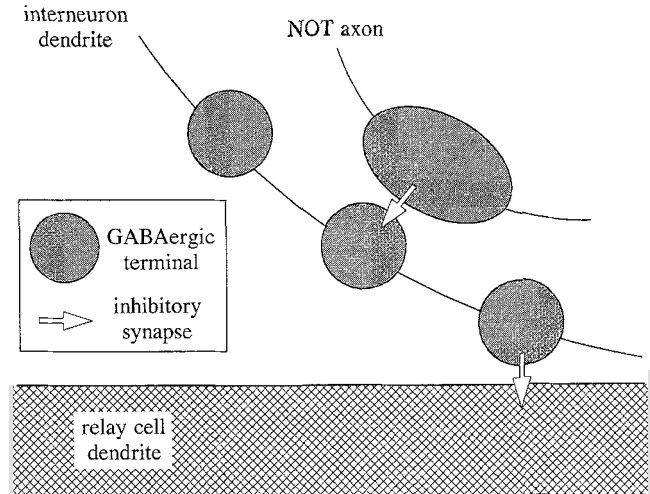


Fig. 13. Schematic summary diagram of circuitry inferred from our observations. An NOT axon forms an inhibitory, GABAergic synapse onto a vesicle-containing, beaded profile of a geniculate interneuron that, in turn, forms an inhibitory, GABAergic synapse onto the dendrite of a geniculate relay cell. In this schema, the pretectal axon inhibits the inhibitory local circuit neuron and thereby facilitates relay cell transmission by disinhibition.

Functional circuitry entered into by NOT afferents

If these main targets of NOT terminals are indeed F2 terminals, then they are dendritic specializations of interneurons that represent a major output of these local circuit cells. We thus conclude that the main target of NOT afferents in the lateral geniculate nucleus is interneurons rather than relay cells. Since the interneurons do provide an inhibitory input to relay cells, particularly via their F2 terminals (Fitzpatrick et al., '84; Wilson et al., '84; Hamos et al., '85; Montero and Singer, '85), the major influence of NOT afferents onto relay cells would be indirect and carried through interneurons. Figure 13 schematically depicts the neural circuitry involving these NOT afferents.

Figure 13 implies that the target profiles of NOT terminals do not form synaptic outputs, but rather the postsynaptic effects are transmitted to a nearby profile joined to the F2-like target profile by the thin connective. For this to work, there must be significant current flow between nearby F2-like profiles. One may wonder if such current flow is plausible over the thin connectives, because in a recent cable model of interneurons, Bloomfield and Sherman ('89) pointed out that nearby clusters of F2 terminals are effectively isolated electrically from one another. However, this cable analysis actually indicates rather little attenuation of current flow for clusters of F2 terminals linked by the same connective (see Fig. 4 of Bloomfield and Sherman, '89): most of the electrical isolation is between clusters, not within them. This is because the slender connectives are one of four factors responsible for this isolation, the others being the large size of the interneuron's dendritic arbor, the failure of dendritic branching to adhere to the "3/2 power rule," and the large number of dendritic branches. It thus seems plausible to conclude that the circuit suggested by Figure 13 would operate fairly effectively.

The function suggested by Figure 13 is that NOT inputs disinhibit relay cells. That is, because most or all NOT terminals are GABAergic and provide inhibitory synaptic output, which is consistent with their F1 morphology and with prior light microscopic studies of the pathway from the NOT to lateral geniculate nucleus (Cucchiaro et al., '91a), they presumably inhibit interneurons. This, in turn, serves to remove inhibition from interneurons to relay cells. Furthermore, NOT axons also innervate the perigeniculate nucleus. Since, like interneurons, perigeniculate axons also provide an inhibitory, GABAergic input to relay cells (Cucchiaro et al., '91b), this provides another route for the NOT to disinhibit relay cells. Montero and Singer ('85) found that many F2 terminals in the cat's lateral geniculate nucleus are postsynaptic to GABAergic F1 terminals, which they presumed were terminals of perigeniculate axons. If so, then the pathway from NOT to perigeniculate cells to F2 terminals of interneurons to relay cells sets up a chain of inhibitory synapses that would enhance inhibition of relay cells: NOT cells would inhibit perigeniculate cells, which disinhibits interneurons, which then further inhibits relay cells. However, Cucchiaro et al. ('91b) found that none of their sample of labeled perigeniculate axons contacted F2 terminals, although many unlabeled F1 terminals did so. It thus seems reasonable to conclude that many or all of the GABAergic F1 terminals contacting F2 terminals as described by Montero and Singer ('85) actually derived from NOT axons. We thus conclude that the projection from the NOT to interneurons and perigeniculate cells serves chiefly to disinhibit relay cells, and this hypothesis is amenable to physiological verification.

The other major brainstem input to the perigeniculate and lateral geniculate nuclei that has been extensively studied is that from cholinergic neurons in the parabrachial region. It is interesting that this pathway also serves to depolarize relay cells, and part of this also seems to be via disinhibition. That is, cholinergic inputs to interneurons and perigeniculate cells seem to hyperpolarize them. In addition, parabrachial axons directly innervate relay cells, which NOT axons do not seem to do, and the relay cells are depolarized by this parabrachial input. Parabrachial axons seem to achieve this different postsynaptic effect by operating through different cholinergic postsynaptic receptors (McCormick and Prince, '86, '87; McCormick and Pape, '88; Hu et al., '89a,b) that can either hyperpolarize or depolarize the cell. The net effect is that both pathways, NOT and parabrachial, act to depolarize relay cells, although their modes of action and anatomical circuitry differ.

ACKNOWLEDGMENTS

This work was supported by NIH grant EY03604.

LITERATURE CITED

- Adams, J.C. (1977) Technical considerations on the use of horseradish peroxidase as a neuronal marker. *Neuroscience* 2:141-145.
- Bloomfield, S.A., and S.M. Sherman (1989) Dendritic current flow in relay cells and interneurons of the cat's lateral geniculate nucleus. *Proc. Natl. Acad. Sci. USA* 86:3911-3914.
- Burke, W., and A.M. Cole (1978) Extraretinal influences on the lateral geniculate nucleus. *Rev. Physiol. Biochem. Pharmacol.* 80:105-166.
- Cucchiaro, J.B., D.J. Uhrlich, and S.M. Sherman (1988) Parabrachial innervation of the cat's dorsal lateral geniculate nucleus: An electron microscopic study using the tracer *Phaseolus vulgaris* leucoagglutinin (PHA-L). *J. Neurosci.* 8:4576-4588.
- Cucchiaro, J.B., D.J. Uhrlich, and S.M. Sherman (1990) A projection from the thalamic reticular nucleus to the dorsal lateral geniculate nucleus in the cat: A comparison with the perigeniculate projection. *Soc. Neurosci. Abstr.* 16:159.
- Cucchiaro, J.B., M.E. Bickford, and S.M. Sherman (1991a) A GABAergic projection from the pretectum to the dorsal lateral geniculate nucleus in the cat. *Neuroscience* 41:213-226.
- Cucchiaro, J.B., D.J. Uhrlich, and S.M. Sherman (1991b) An electron-microscopic analysis of synaptic input from the perigeniculate nucleus to the A-laminae of the lateral geniculate nucleus in the cat. *J. Comp. Neurol.* 310:316-336.
- Eldred, W.D., C. Zucker, H.J. Karten, and S. Yazulla (1983) Comparison of fixation and penetration enhancement techniques for use in ultrastructural immunohistochemistry. *J. Histochem. Cytochem.* 31:285-292.
- Fitzpatrick, D., G.R. Penny, and D.E. Schmechel (1984) Glutamic acid decarboxylase-immunoreactive neurons and terminals in the lateral geniculate nucleus of the cat. *J. Neurosci.* 4:1809-1829.
- Graybiel, A.M., and D.M. Berson (1980) Autoradiographic evidence for a projection from the pretectal nucleus of the optic tract to the dorsal lateral geniculate complex in the cat. *Brain Res.* 195:1-12.
- Guillery, R.W. (1969a) The organization of synaptic interconnections in the laminae of the dorsal lateral geniculate nucleus of the cat. *Z. Zellforsch.* 96:1-38.
- Guillery, R.W. (1969b) A quantitative study of synaptic interconnections in the dorsal lateral geniculate nucleus of the cat. *Z. Zellforsch.* 96:39-48.
- Hamos, J.E., S.C. Van Horn, D. Raczkowski, D.J. Uhrlich, and S.M. Sherman (1985) Synaptic connectivity of a local circuit neuron in lateral geniculate nucleus of the cat. *Nature* 317:618-621.
- Hamos, J.E., S.C. Van Horn, D. Raczkowski, and S.M. Sherman (1987) Synaptic circuits involving an individual retinogeniculate axon in the cat. *J. Comp. Neurol.* 259:165-192.
- Hu, B., M. Steriade, and M. Decshènes (1989a) The effects of brainstem peribrachial stimulation on perigeniculate neurons: The blockage of spindle waves. *Neuroscience* 31:1-12.
- Hu, B., M. Steriade, and M. Decshènes (1989a) The effects of brainstem peribrachial stimulation on neurons of the lateral geniculate nucleus. *Neuroscience* 31:13-24.
- Kubota, T., M. Morimoto, T. Kanaseki, and H. Inomata. (1987) Projection from the pretectal nuclei to the dorsal lateral geniculate nucleus in the cat: A wheatgerm agglutinin-horseradish peroxidase study. *Brain Res.* 421:30-40.
- Kubota, T., M. Morimoto, T. Kanaseki, and H. Inomata (1988) Visual pretectal neurons projecting to the dorsal lateral geniculate nucleus and pulvinar nucleus in the cat. *Brain Res. Bull.* 20:573-579.
- McCormick, D.A., and D.A. Prince (1986) Acetylcholine induces burst firing in thalamic neurones by activating a potassium conductance. *Nature* 319:402-405.
- McCormick, D.A., and D.A. Prince (1987) Actions of acetylcholine in the guinea pig and cat medial and lateral geniculate nuclei, in vitro. *J. Physiol. (Lond.)* 392:147-165.
- McCormick, D.A., and H.C. Pape (1988) Acetylcholine inhibits identified interneurons in the cat lateral geniculate nucleus. *Nature* 334:246-248.
- Montero, V.M. (1987) Ultrastructural identification of synaptic terminals from the axon of type 3 interneurons in the cat lateral geniculate nucleus. *J. Comp. Neurol.* 264:268-283.
- Montero, V.M., and W. Singer (1985) Ultrastructural identification of somata and neural processes immunoreactive to antibodies against glutamic acid decarboxylase (GAD) in the dorsal lateral geniculate nucleus of the cat. *Exp. Brain Res.* 59:151-165.
- Sherman, S.M., and C. Koch (1986) The control of retinogeniculate transmission in the mammalian lateral geniculate nucleus. *Exp. Brain Res.* 63:1-20.
- Sherman, S.M., and C. Koch (1990) Thalamus. In G.M. Shepherd (ed): *Synaptic Organization of the Brain*, 3rd ed. New York: Oxford, pp. 246-278.
- Singer, W. (1977) Control of thalamic transmission by corticofugal and ascending reticular pathways in the visual system. *Physiol. Rev.* 57:386-420.
- Steriade, M., and R.R. Llinás (1988) The functional states of the thalamus and the associated neuronal interplay. *Physiol. Rev.* 68:649-742.
- Wilson, J.R., M.J. Friedlander, and S.M. Sherman (1984) Fine structural morphology of identified X- and Y-cells in the cat's lateral geniculate nucleus. *Proc. R. Soc. Lond. [Biol.]* 221:411-436.